A uW Backscatter-Morse-Leaf Sensor for Low-Power Agricultural Wireless Sensor Networks

Daskalakis, S. N., Goussetis, G., Assimonis, S. D., Tentzeris, M. M., & Georgiadis, A. (2018). A uW Backscatter-Morse-Leaf Sensor for Low-Power Agricultural Wireless Sensor Networks. *IEEE Sensors Journal*, *18*(19), 7889-7898. https://doi.org/10.1109/JSEN.2018.2861431

Published in:
IEEE Sensors Journal

Document Version:
Peer reviewed version

A uW Backscatter-Morse-Leaf Sensor for Low-Power Agricultural Wireless Sensor Networks

Spyridon N. Daskalakis, *Student Member, IEEE*, George Goussetis, *Senior Member, IEEE*, Stylianos D. Assimonis, Manos M. Tentzeris, *Fellow, IEEE* and Apostolos Georgiadis, *Senior Member, IEEE*

***Abstract*—Nowadays, the monitoring of plant water stress is of high importance in smart agriculture. Instead of the traditional ground soil-moisture measurement, leaf sensing is a new technology, which is used for the detection of plants needing water. In this work, a novel, low-cost and low-power system for leaf sensing using a new plant backscatter sensor node/tag is presented. The latter, can result in the prevention of water waste (water-use efficiency), when is connected to an irrigation system. Specifically, the sensor measures the temperature differential between the leaf and the air, which is directly related to the plant water stress. Next, the tag collects the information from the leaf sensor through an analog-to-digital converter (ADC), and then, communicates remotely with a low-cost software-defined radio (SDR) reader using monostatic backscatter architecture. The tag consists of the sensor board, a microcontroller, an external timer and an RF front-end for communication. The timer produces a subcarrier frequency for simultaneous access of multiple tags. The proposed work could be scaled and be a part of a large backscatter wireless sensor network (WSN). The communication protocol exploits the low-complexity Morse code modulation on a 868 MHz carrier signal. The presented novel proof-of-consent prototype is batteryless and was powered by a flexible solar panel consuming power around 20 μW. The performance was validated in an indoors environment where wireless communication was successfully achieved up to 2 m distance.**

***Index Terms*—Backscatter sensor networks, environmental monitoring, Internet-of-Things (IoT), leaf sensor, Morse code, precision agriculture, radio frequency identification (RFID) sensors, software-defined radio (SDR).**

I. Introduction

Precision agriculture allows farmers to maximize yields using minimal resources such as water, fertilizer, pesticides and seeds. By deploying sensors and monitoring fields, farmers can manage their crops at micro scale [1]. This is also useful in order to predict diseases, conserve the resources and reduce the impacts of the environment. During the 1990s, early precision agriculture users adopted crop yield monitoring to generate fertilizer and pH correction recommendations. As more variables could be measured by sensors and were introduced into a crop model, more accurate recommendations could be made. The combination of the aforementioned systems with wireless sensor networks (WSNs) allows multiple unassisted embedded devices (sensor nodes) to transmit wirelessly data to central base stations [2], [3]. The base stations are able to store the data into cloud databases for worldwide processing and visualization [4]. Data (e.g., temperature, humidity, pressure) are collected from different on-board physical sensors: dielectric soil moisture sensors, for instance, are widespread for moisture measurements, since they can estimate the moisture levels through the dielectric constant of the soil, which changes as the soil moisture is changing.

Leaf sensing is an another way to measure the water status of a plant. When compared to soil moisture sensors, they can provide more accurate data since the measurements are directly taken on the plant and not through the soil or the atmosphere (air), which surround the latter [5]. Commercial leaf sensors are involve phytometric devices that measure the water deficit stress (WDS) by monitoring the moisture level in plant leaves. In recent work [6], a leaf sensor is used to measure the plant's leaf thickness in order to determine the WDS. The sensor is provided by AgriHouse Inc. and it is suitable for real-time monitoring in aeroponics, hydroponics and drip irrigation systems [7]. In an extreme WDS scenario, the leaf thickness decreased dramatically (by as much as 45%) within a short period of time (2 hours). On other occasions, the leaf thickness was kept fairly constant for several days, but decreased substantially when WDS became too severe for the plant [6]. Despite such favourable features, this class of sensors can only be used in controlled environments (i.e., greenhouses) in combination with other type of sensors. This is because a direct relationship seems to exist between leaf thickness and the relative humidity of the ambient air, temperature, soil temperature and soil salinity [6].

A different type of leaf sensor for WDS monitoring, is described in [5] and is using two temperature sensors. The monitoring is based on the temperature difference between the leaf and the air ($T_{\text{leaf}} - T_{\text{air}}$). This difference is strictly related to the plant water stress and can be used as decision parameter in a local irrigation system [8]. The first sensor measures the canopy temperature on the leaf (T_{leaf}) and the second the atmospheric temperature (T_{air}). The use of

This work was supported by Lloyd's Register Foundation (LRF) and the International Consortium in Nanotechnology (ICON). The work of M. M. Tentzeris was supported by the National Science Foundation (NSF) and the Defense Threat Reduction Agency (DTRA).

An earlier version of this paper was presented at the IEEE Sensors Conference, Glasgow, United Kingdom, 29 Oct - 01 Nov 2017 and was published in its Proceedings. Conference version of this paper is available online at http://ieeexplore.ieee.org/document/8233888/.

S. N. Daskalakis, G. Goussetis and A. Georgiadis are with School of Engineering & Physical Sciences; Institute of Sensors, Signals and Systems, Heriot-Watt University, Edinburgh, EH14 4AS, Scotland, UK (e-mail: sd70@hw.ac.uk, g.goussetis@hw.ac.uk, apostolos.georgiadis@ieee.org).

S. D. Assimonis is with School of Electronics, Electrical Engineering & Computer Science, Queen's University Belfast, Belfast, BT3 9DT, UK (e-mail: s.assimonis@qub.ac.uk).

M. M. Tentzeris is with School of Electrical and Computer Engineering, Georgia Institute of Technology, Atlanta, GA, 30332-250, USA (e-mail: etentze@ece.gatech.edu).

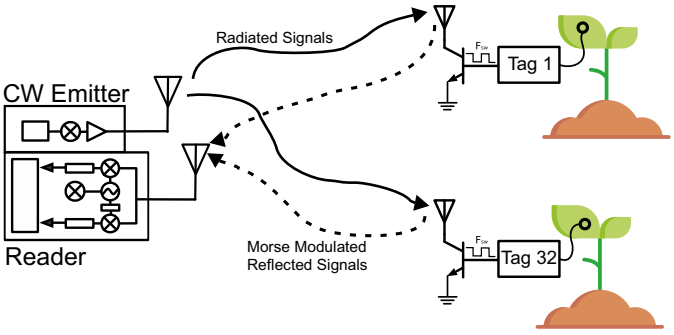

Fig. 1. Monostatic backscatter communication setup. Plant sensing is achieved by the tags and the information is sent back to a low-cost reader. Information is modulated using Morse coding on a 868 MHz radiated carrier.

canopy temperature as an indicator of crop water stress has been the subject of much research over the past 30 years [9]. Canopy temperature and water stress are related: when the soil moisture is reduced, stomatal closure occurs on the leaves resulting to reduced transpirational cooling. The canopy temperature is then increased above that of the air [10]. In a plant with adequate water supply, the term $T_{\text{leaf}} - T_{\text{air}}$ will be zero or negative, but when the available water is limited, the difference will be positive.

The leaf sensors that were described above are different from the well known leaf wetness sensors (LWS). The LWS can detect the leaf wetness which is a meteorological parameter that describes the amount of dew and precipitation left on leaf surfaces. Leaf wetness can result from dew, fog, rain, and overhead irrigation. Today, the LWS are used most for disease-warning systems [11] and provided by companies like Davis Instruments Inc. and Meter Environment Inc. [12].

The agricultural applications frequently involve large, expansive areas where wire connection for communication and power is undesirable or impracticable [2]. The high-cost and the high-power requirements of the today WSN hardware prevent its usage in agriculture. The deployment of these systems therefore relies on reducing the cost to an affordable amount. Capital expenditure relates to the cost of the hardware, which should therefore be maintained minimum. Energy autonomy for the sensor achieved by a combination of minimizing power consumption and harvesting ambient energy is likewise critical in order to reduce operational costs. Above factors drive the demand for low-cost, low-power WSN systems.

Backscatter radio communication (i.e., reflection and modulation of an incident radio frequency carrier) in combination with the use of energy assisted (or not) sensor tags is a method that addresses aforementioned constraints. It is used in radio frequency identification (RFID) applications and offers ultra-low-power and low-cost aspects [13]. The wireless communication part of each tag can be simplified into a single radio frequency (RF) transistor and an antenna, which can be used for each sensor tag to send information to a base station (reader). It is a very energy-efficient communication technique thus the RF signal is used not only for the communication, but also, for the power of the tag [14]. In the recent literature, backscatter WSNs for smart agriculture purposes [15]–[18] were proposed. In [15], [16], soil moisture and humidity sensors were proposed. A proof of concept demonstration was presented where the tags send measurements to a software-defined radio (SDR) reader. The WSNs employ semi-passive tags in bistatic topology and each backscatter sensor tag has power consumption of the order of 1 mW. The achieved communication range (tag-reader distance) is of the order of 100 m; this is achieved by supplying the tags with small batteries thereby enabling increased communication range. In [17], electric potential (EP) signals of plants can be measured by the tag in order to estimate when the plant needs water; in this work, the tags are batteryless and they harvest energy from the plant itself. In [18] two UHF RFID sensor nodes for soil moisture sensing were designed based on conventional RFID chips.

This work discusses the implementation of a low-cost and low-power wireless sensor system for agricultural applications, which uses a novel plant, backscatter sensor node/tag. Preliminary results on this sensor node were proposed in [19]. The tag is connected with a temperature leaf sensor board for WDS measurements and reflects RF signals from a carrier emitter. It is noted that the proposed system can be a part of a backscatter WSN, transmitting data to a reader as shown in Fig. 1. Specifically the tag architecture consists of a microcontroller (MCU) and an external timer for the modulation. There is also a sensor board for the measurements and an FR front-end for the backscatter communication. The tag reads the information from the sensors and generates pulses that control an RF switch.

The low complexity Morse code technique was selected for the backscatter modulation and it is the first time that Morse code is used in a backscatter WSN system. Morse code uses On-Off-Keying (OOK) modulation which means that a frequency signal exists in only two states either “On” or “Off”. Morse code and OOK contribute to architectural and power consumption efficiencies for the tag. A low-cost SDR is used as reader and collects the signals for further processing. The 868 MHz in the European RFID band was selected as carrier emitter frequency.

The structure of the this paper is as follows: Section II provides the basic principles of backscatter communication and the Morse encoding. In Section III the design and the implementation of the tag is described. Section IV discusses the hardware and software part of the low-cost receiver. Section V presents the proof-of-concept experimental setup and a communication indoor demo. In Section VI, the benefits of our proposed low-power WSN and future work are discussed. Finally, section VII includes concluding remarks.

II. Backscatter and Morse Encoding

A typical backscatter communication system requires three devices: a tag, an emitter and a reader. Traditional batteryless RFID systems utilize monostatic architectures, where the reader and the emitter are in the same box. In this work this architecture is employed; the emitter transmits a continuous wave (CW) signal at frequency F_c = 868 MHz. The tag receives and scatters a fraction of it back to the reader as

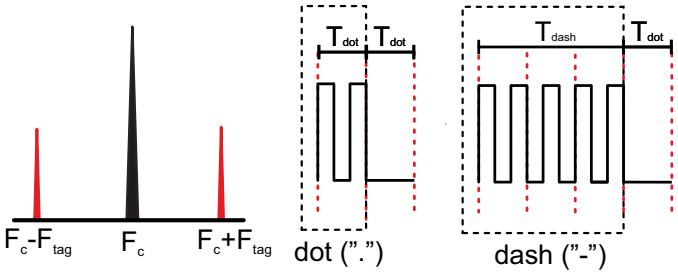

Fig. 2. Left: In Backscatter principle when a F_c carrier exists and the RF switch frequency is F_{tag}, two subcarriers appear with frequencies $F\text{c} \pm F_{\text{tag}}$. Right: Morse code symbols.

shown in Fig. 1. The backscatter binary communication can be implemented on the tag using an RF switch, an antenna and a control unit. The switch alternates the load of the antenna between two values ($Z_{1/2}$) and offers two reflection coefficients, ($\Gamma_{1/2}$), according to

$$\Gamma_{1/2} = \frac{Z_{1/2} - Z_{\text{a}}^*}{Z_{1/2} + Z_{\text{a}}}, \tag{1}$$

with Z_{a}, the antenna impedance equal with 50 Ohm. When the CW with frequency F_{c} arrives on the antenna and the RF switch frequency is F_{tag}, frequency modulation occurs and two subcarriers appear in the spectrum with frequencies $F_{\text{sub1/2}} = F_{\text{c}} \pm F_{\text{tag}}$. The reflected signal (subcarriers) and the carrier are depicted in Fig. 2 (left). The subcarriers are next modulated using the Morse code scheme as it is described below.

Morse code is a method of transmitting text information as a series of On-Off tones, named after the inventor of the telegraph Samuel F. B. Morse in the 1830s [20]. It is referred as the earliest type of binary digital communications since the code is made solely from ones and zeros (“On” and “Off”). Each letter of the alphabet is translated to combinations of dots “.” and dashes “-” that are sent over telegraph wires or by radio waves from one place to another. For example, the letter “A” is translated to the sequence “.-” with elements one dot and one dash symbol. Lets assume that the duration of a dot (T_{dot}) is one unit, then the duration a dash is three units ($3T_{\text{dot}}$). Dot and dash symbols are followed by a short silence, equal to one unit (Fig. 2, right). The space between the elements of one letter/character is one unit, between characters is three units and between words, seven units.

The Morse code is the only digital modulation designed to be easily read without a computer. Today it is usually used by radio amateurs and it is the fist time that is used in backscatter communication. The OOK modulation is used to transmit Morse code signals over a fixed radio frequency. The OOK is a simplest form of amplitude-shift keying (ASK) modulation that can represent digital data using a presence (“On”) or an absence (“Off”) of a carrier signal. With OOK modulation and thus Morse code, the complexity of the receiver and the tag is drastically simplified compared to a frequency modulation (FM) scheme thus there is no need for a different frequency for each symbol [21]. Also, Morse code was designed so that the most frequently used letters have the shortest codes. In general, code length increases as frequency decreases.

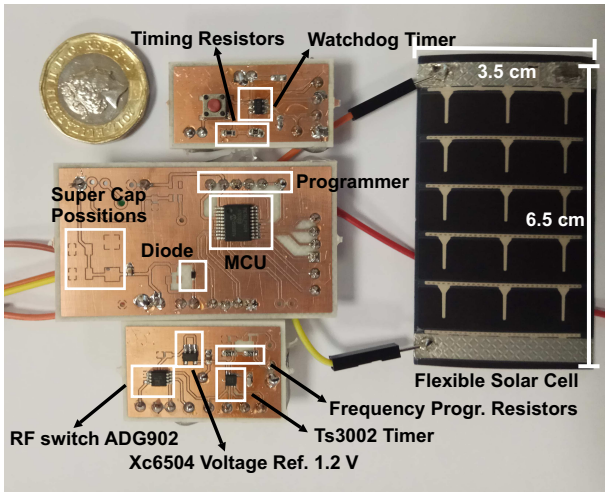

Fig. 3. Printed circuit boards of the tag and the solar cell. The watchdog timer (top) and the timer module (bottom) are connected with the main processor unit in the middle.

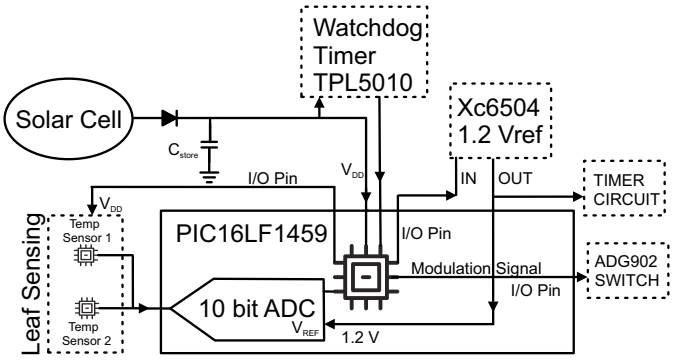

Fig. 4. The schematic of the tag’s main unit. The main part, is a low-power MCU that controls the sensors, the timer and the RF front-end.

In this work the “.” (dot of Morse code) is implemented as a signal with a specific duration T_{dot} and frequency F_{tag}. As it is expected the “-” (dash in Morse code) is then implemented using a signal of the same frequency with duration equal to three times that of the dot signal. The T_{dot} is defined by the MCU and the F_{tag} is defined by the external timer of the tag. The dot and dash frequency signals are shown in Fig. 2 (left). The speed of Morse code is stated in words per minute (WPM) and according to the standards, the word PARIS is used to determine it. The word is translated to exactly 50 units and one dot duration is defined by the formula: $T_{\text{dot}} = 1200/\text{WPM}$ with T_{dot} in ms.

III. Tag Implementation

A. Main Unit

The proof-of-concept tag consists of five different parts implemented in different printed circuit boards (PCBs) for simplifying debugging. These parts are the MCU unit, the timer part, the watchdog timer part, the sensor board, and finally the RF front-end. The MCU unit (Fig. 3, middle) is the main part of the system and it is responsible for the data sensor acquisition, the implementation of the Morse code

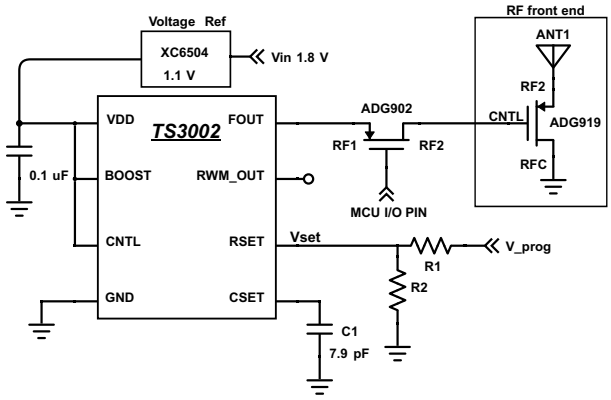

Fig. 5. Timer and RF front-end schematic of the tag. The timer produces square wave pulses with 50% duty circle and supplies the RF front-end through a modulation switch (ADG902). The ADG902 switch is controlled by the MCU.

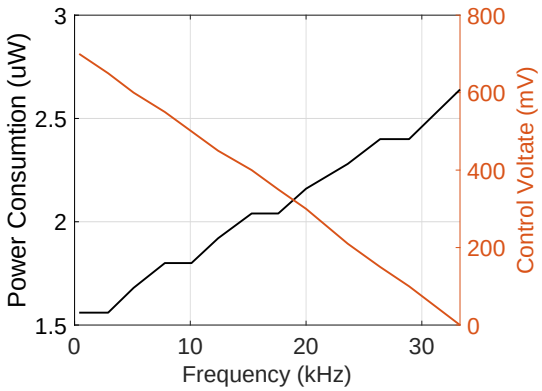

Fig. 6. Power consumption of the TS3002 timer versus the output frequency (F_{tag}) versus the control voltage V_{prog}.

symbols and the control of the other parts. The schematic of the main system is depicted in Fig. 4. The ultra-low-power 8-bit PIC16LF1459 from Microchip with current consumption of only 25 μA/MHz at 1.8 V [22] was selected for the MCU. The MCU collects data from the sensor board using the embedded analog-to-digital converter (ADC) with 10-bit resolution. It contains also a digital-to-analog converter (DAC) with 5-bit resolution. The internal 31 kHz low-power oscillator was utilized as clock source in order to reduce the power consumption of the tag. The MCU is responsible to supply all the other parts with voltage when it is necessary. The main part is connected with a μW timer for the subcarrier signal (F_{tag}) production and an external watchdog timer to wake up the MCU from the "sleep" operation mode. In sleep mode the MCU current consumption was only 0.6 μA at 1.8 V.

B. Timers

The timer module (Fig. 3, bottom) consists of a very low-power timer (TS3002), a voltage reference and a switch. It is responsible for producing the subcarrier frequency of the tag F_{tag} and modulating this subcarrier through the switch. The low-power, single-pole single-throw (SPST) switch ADG902 was used in this case and one of the MCU input/output (I/O) pins was programmed to provide the necessary Morse code pulses for the control. The implemented circuit is depicted in Fig. 5. The TS3002 is a CMOS oscillator provided by Silicon Labs Inc., fully specified to operate at around 1 V and to consume current lower than 5 μA with an output frequency range from 5.2 kHz to 290 kHz [23]. The timer was supplied by a voltage reference integrated circuit (IC) XC6504 at 1.2 V [24] in order to reduce the power consumption. XC6504 provides also stable reference voltage at the ADC of the tag and it is activated by an I/O pin of MCU. The output frequency of the timer is programmed by using two parallel external resistors, a capacitor and a voltage value. The square wave pulses have 50 % duty cycle and the maximum oscillation frequency when a zero voltage is applied at V_{prog}, is given by

$$F_{\text{tag,max}} = \frac{1}{1.19 C_1 R_{\text{set}}}, \tag{2}$$

with $R_{\text{set}} = R_1 R_2/(R_1 + R_2)$. In our proof-of-concept prototype two identical resistors were used with value of 6.2 MOhm and tolerance 1% in order to avoid the frequency jitter. The output frequency was programmed to 34.3 kHz and the power consumption of the timer circuit was measured at 2.62 uW. The above measurement includes the power consumption of the voltage reference IC. The TS3002 can be configured as a voltage controlled oscillator (VCO) by applying a positive voltage value at V_{prog} terminal and the F_{tag} frequency is defined as [25]:

$$F_{\text{tag}} = V_{\text{prog}} \frac{-F_{\text{tag,max}}}{V_{\text{prog,max}}} + F_{\text{tag,max}}, \tag{3}$$

with $V_{\text{prog,max}}$, the maximum value of V_{prog} when the timer gives zero frequency at its output. In Fig. 6 the ultra-low-power consumption of the timer versus different frequencies at the output is shown. Each frequency value corresponds to a different control voltage value (V_{prog}).

In case of a multiple access scheme, we have multiple tags in the same network sending information simultaneously. Each tag must operate in different F_{tag} frequency and the embedded DAC could be used in order to tune every tag in different subcarrier. The DAC can supply the timer with 2^5 distinct voltage levels (V_{prog}) corresponding to 32 distinct subcarriers resulting in 32 tags in the same network. In this work the DAC is not used in order to reduce the overall power consumption of the prototype tag. The subcarrier frequency was programmed manually by using the two resistors and V_{prog} terminal was connected to the ground.

For minimization of the average power consumption, a duty cycle operation of the tag was programmed. The tag was active only for a desired minimum period of time and a watchdog timer was used as a real-time clock (RTC). Specifically, the nano power TPL5010 timer from Texas Instruments [26] was utilized, which consumes only 35 nA. The timer can work as RTC and allows the MCU to be placed in sleep mode. The timer can provide an interrupt signal in selectable timing

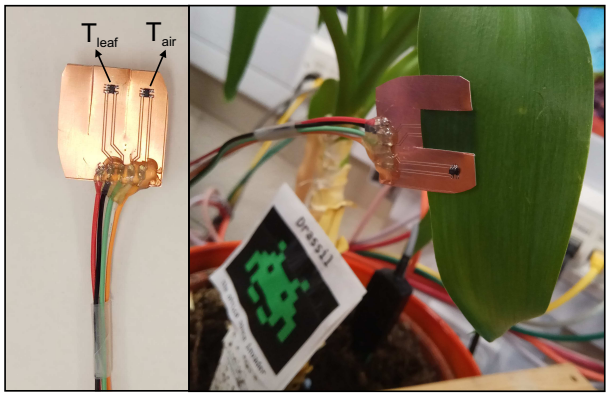

Fig. 7. Printed circuit board with low-power LMT84 temperature sensors. The sensor board can be placed easily on a leaf.

intervals from 0.1 to 7200 s by programming two external parallel resistors. It was programmed to wake up the MCU every 4 s activating the duty cycle operation of the system. The PCB of the watchdog timer is shown in Fig. 3 (top).

C. Sensor Board

The sensor board consists of two analog temperature sensors "LMT84" by Texas Instruments (Fig. 7, left). Each sensor is connected with an ADC input and consumes 5.4 μA at 1.8 V [27]. The accuracy of each one is $\pm 0.4^{\circ}C$, while both were placed on a "clip" scheme board in order to be easily mounted on a leaf. The prototype placed on a leaf is depicted in Fig. 7, (right). The temperature sensor seen on the top measures the air temperature (T_{air}), while a similar sensor under the leaf surface is placed in direct contact with the leaf and measures the canopy temperature T_{leaf}. The transfer function of the each sensor is defined as [27]:

$$T_{\text{leaf/air}} = \frac{5.506 - \sqrt{36.445 - 0.00704 V_{\text{leaf/air}}}}{-0.00352} + 30, \qquad (4)$$

where $V_{\text{leaf/air}}$ is the ADC value in mV and $T_{\text{leaf/air}}$ is temperature in $^{\circ}C$. The MCU collects data from sensors one by one in order to minimize the instantaneous power consumption. The two ADC measurements were encoded using the Morse code and were sent back to the receiver. At the receiver, the signal from both sensors is decoded in terms of a voltage value (in mV) and the temperature is then calculated using formula (4). Subsequently, the temperature difference $T_{\text{leaf}} - T_{\text{air}}$ is estimated and recorded.

D. RF Front-end

The RF front-end part consists of an RF switch and a custom dipole antenna as it is depicted in Fig. 8 (bottom). The RF front-end is connected to the ADG902 switch of the timer module (Fig. 5). It is used for the wireless communication with the reader and it it responsible for creating the reflections of the incident CW signal. The single-pole, double-throw (SPDT) switch ADG919 [28] was selected due to its low insertion loss and high "OFF" isolation. The "RFC" and the "RF2" terminals of the RF switch were connected to the two arms of dipole antenna. The dipole antenna has omnidirectional attributes at

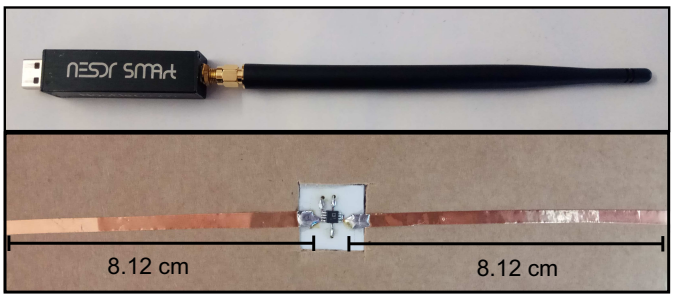

Fig. 8. Top: Low-cost software-defined radio. Bottom: RF front-end board with ADG919 switch.

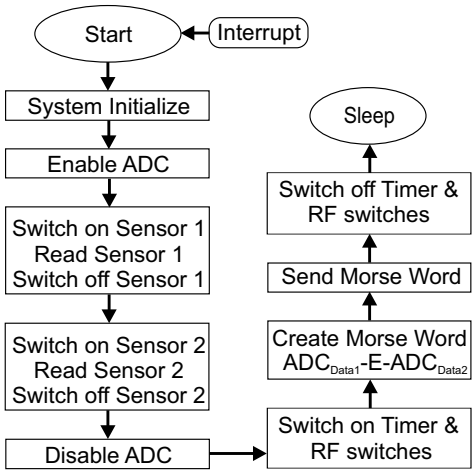

Fig. 9. Flow chart of the tag algorithm. This algorithm was implemented in the MCU and controls all the peripherals of the tag.

the vertical to its axis level and was designed for operation at 868 MHz. The bottom picture of Fig. 8 shows the fabricated prototype and the dimensions of the antenna. The RF Front-end was fabricated using copper tape on cardboard substrate.

E. Tag Analysis

In this work a solar panel harvester was employed for powering the tag. Solar energy could be used to power the tag also in combination with other energy harvesting technologies [29]. This solar module is the flexible, thin-film SP3-37 provided by PowerFilm Inc. [30]. The solar panel charges a 11 mF super capacitor (CPH3225A) instead of a battery through a low voltage drop Schottky diode. For the diode, the SMS7630-079LF by Skyworks Inc. with forward voltage drop only 150 mV was selected. The solar panel, the diode and the capacitor positions are depicted in Fig. 3.

On the tag, a real-time algorithm was implemented in order to read the sensor information and wirelessly transmit it to the receiver. The steps of the algorithm are shown in Fig. 9. Initially, an interrupt signal coming from the watchdog timer is used to wake up the MCU. Next, initialization of the system (ADC, clock, I/O pins) is achieved and the ADC is enabled for data capture. The two temperature sensors are consecutively powered and the ADC reads the data from each one. The ADC is turned off immediately after this action for reducing the energy consumption. In the next step, the

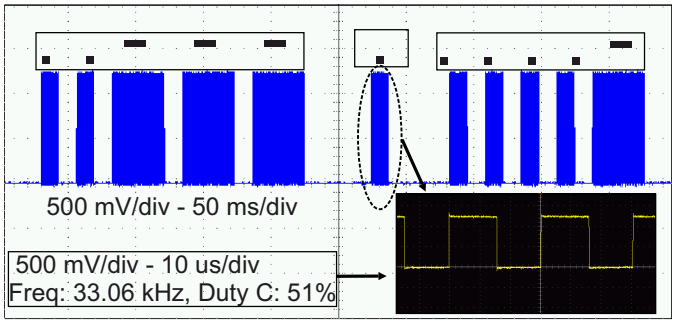

Fig. 10. Oscilloscope measurement of a Morse coded word: ". . - - - . . . . -" corresponding to "2**E**4" word. This square wave signal is used to control the RF front-end.

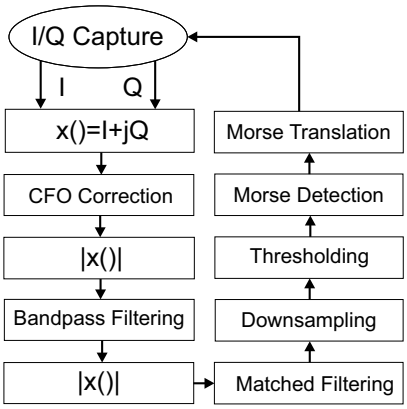

Fig. 11. Flow chart of the real-time receiver algorithm. The decoding algorithm was implemented in MATLAB software.

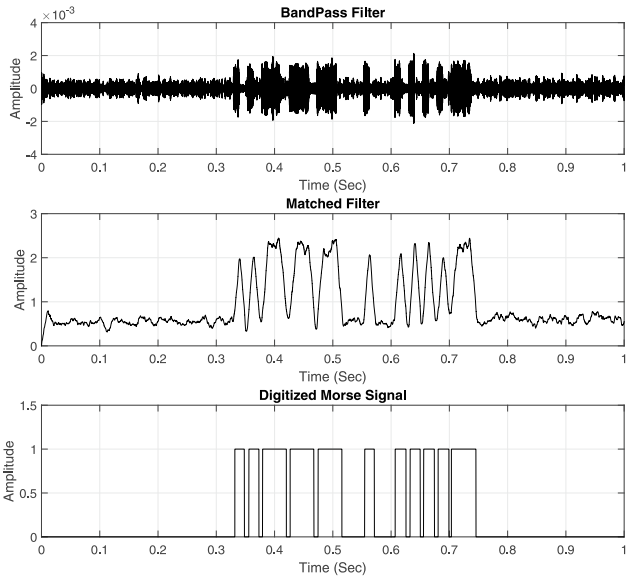

Fig. 12. A received signal including a Morse coded word in three different steps of decoding algorithm.

TS3002 timer and the ADG902/919 switches are switched on two steps before the data sending. This is necessary for the frequency stabilization of the timer. The tag was programmed to send a Morse coded word with fixed format every time the algorithm is running. The format of the word was defined as "ADC_{DATA1}**E**ADC_{DATA2}" with ADC_{DATA1}, ADC_{DATA2}, the ADC values, varied for 0 to 1023. The sensor data were separated by the letter "E" and there are not any spaces between them. The goal was to create a short word to minimize the transmission time and thus the energy consumption. The letter "E" is the most common letter in English alphabet and has the shortest code, a single dot. The word is then translated in dots and dashes using the frequency F_{tag} of the timer and baseband pulses coming from the MCU.

The MCU produces baseband pulses that contain the dots, dashes and the spaces between them. This signal is coming from an I/O pin and is used to modulate the timer's frequency signal through the ADG902 switch. In Fig. 10 an oscilloscope measurement of a modulated example signal at the output of ADG902 switch is shown. The depicted word is the "2**E**4" which is translated in ". . - - - . . . . -", while each dot/dash is a 33 kHz signal with different duration. The required spaces between the Morse code symbols can also be observed. In order to send this word wirelessly, the RF switch ADG919 is fed with this signal and the incident CW carrier is modulated again by the tag information. In the last step of the algorithm, the switches and the timer were switched off and the tag goes to sleep mode. The time duration of the algorithm depends from the ADC data and the worst-case scenario is the word "1023**E**1023". In that case the duration of the hole process lasts 2.8 s assuming 104.3 WPM speed.

IV. Receiver

In our system the temperature ADC data are received by a low-cost SDR. This receiver is the "NESDR SMArt" SDR available by the NooElec Inc. (Fig. 8, top) [31]. It is an improved version of classic RTL SDR dongle based on the same RTL2832U demodulator with USB interface and R820T2 tuner. The tuning frequency range varies from 24 MHz to 1850 MHz with sampling rate up to 2.8 MS/s and noise figure about 3.5 dB. Gain control is also provided through the embedded low noise amplifier (LNA) at the input of R820T2, while at the output through a variable gain amplifier (VGA). It down-converts the received RF signal to baseband and it sends real (I) and imaginary (Q) signal samples to a computer through an USB interface. All the above parameters make it suitable for our application also noting that the required sampling rate is quite low (250 kS/s) and it costs only 12.8 GBP. The receiver was connected with a 868 MHz monopole antenna to receive the signals from the tag.

A real-time algorithm was implemented in MATLAB in order to detect the reflected signals. The SDR can be connected with MATLAB through the open course GNU radio framework [32]. In the algorithm, the subcarrier frequency F_{tag} of the tag is known and the algorithm collects data in a window with duration: 2×length(maximum word). As shown in Fig. 11, the received I and Q digitized samples were combined together in complex numbers. Carrier frequency offset (CFO) was estimated and the signal was corrected. This accounts for the difference in carrier frequency between the SDR and the emitter, providing the variance between the real values and the estimated values of the subcarrier signal. The CFO

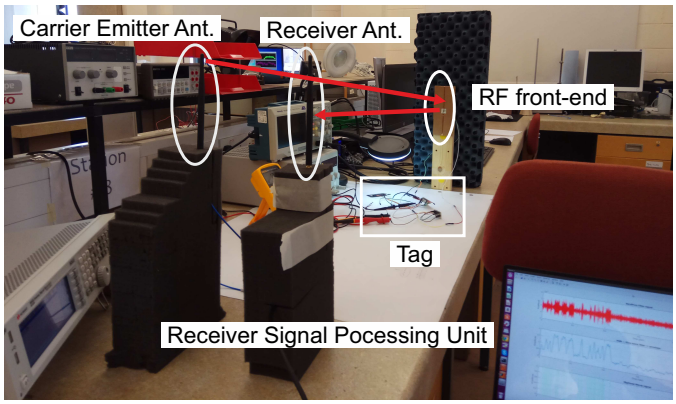

Fig. 13. Experimental indoor backscatter topology. The tag was measured in monostatic architecture 2 m away from emitter and receiver antennas.

was estimated after the samples were collected and then all samples were frequency shifted accordingly. The absolute value is taken and a bandpass filter with center frequency F_{tag} is applied in order to appear the Morse code word. After considering the signal magnitude, a matched filter was applied to appear the baseband Mode symbols. The matched filter is a square pulse with duration T_{dot}. The received signal of the Fig. 10 word is shown in Fig. 12, (a) after the Band-pass filtering. In Fig. 12, (b) is shown the above signal after matched filtering. The matched filtering was followed by downsampling with a factor of 100 for reducing of the computational complexity. Next, the received signal must be digitized using a threshold level. AGC (automatic gain control) and threshold decision is needed because the signal strength varies over time. The digitization procedure, which is using a suitable threshold, is depicted in Fig. 12, (c). The digitized signal was classified in order to detect the Morse code symbols and thus the alphabet characters. For the classification, a group of tokens was used with each token to be an English alphabet character translated in dots and dashes. The output of the algorithm is the English text and number representation of the Morse word.

V. Experimental results

The proof-of-concept system was tested indoors in a setup depicted in Fig. 13 in order to validate the effectiveness of our backscatter communication system. The emitter, the tag and the reader were tested in monostatic architecture in Heriot-Watt University electromagnetics lab. A signal generator with a monopole antenna was utilized as the CW emitter at 868 MHz, with a transmission power of 13 dBm. The SDR reader was used as the software-defined receiver in the same position with the emitter. The receiver was tuned to 868 MHz with sampling rate 250 kbps. The distance between the reader and emitter antenna was fixed at 17.27 cm ($\lambda/2$). The tag was placed 2 m away from the emitter/reader antennas and was programmed to produce words with Morse code symbols. Each word contains the T_{leaf} and T_{air} values in mV at 104.3 WPM speed. The sensor node has low-power consumption and was supplied by the solar panel and the super capacitor. An office lamb was used as an indoor source of light. Results shown that the transmitted words can be presented clearly at the receiver.

TABLE I
Tag Current Consumption & Cost Analysis

Tag Part	Cost (GBP)	Current (μA)
MCU (PIC16F1459)	1.44	-
ACTIVE MODE (ADC OFF)	-	3.3 @$V_{\text{DD}} = 1.8$ V
ACTIVE MODE (ADC ON)	-	198.4 @$V_{\text{DD}} = 1.8$ V
SLEEP MODE	-	0.6 @$V_{\text{DD}} = 1.8$ V
Timer (TS3002)	0.54	2.2 @$V_{\text{DD}} = 1.2$ V
Voltage Reference (XC6504)	0.42	0.6 @$V_{\text{DD}} = 1.8$ V
Watchdog timer (TPL5010)	0.93	0.035 @$V_{\text{DD}} = 1.8$ V
RF Switches (ADG902+ADG919)	$2.39 + 2.49$	0.1 @$V_{\text{DD}} = 1.8$ V
Temp Sensors (2×LMT84)	$0.64 + 0.64$	5.3 @$V_{\text{DD}} = 1.8$ V
Super Cap (CPH3225A)	2.05	-
Solar Panel (SP3-37)	2.20	-
Sum	14.16	-
Sum ACTIVE MODE (ADC OFF)	-	11.5 @$V_{\text{DD}} = 1.8$ V
Sum ACTIVE MODE (ADC ON)	-	201 @$V_{\text{DD}} = 1.8$ V
Sum SLEEP MODE	-	0.6 @$V_{\text{DD}} = 1.8$ V

Table I provides cost of the most significant components of the tag and the current consumption of each one. In active mode, the maximum overall dissipated current at 1.8 V was measured 11.5 μA (20.7 μW) when the ADC was off and 201 μA (362 μW) when the ADC was active. In the sleep mode operation the current consumption was 0.6 μA (1 μW). Finally, using discrete electronic components in terms of bill of materials (BOM), the tag results in the cost of 14.1 GBP and the prices of each component were found from online suppliers on the order of one.

Looking at the market, we found only one leaf sensor provided by Agrihouse Inc. It costs 290 USD without the wireless communication equipment and according to the above, this work seems to be a promising low-cost alternative solution in order to monitor the WDS of the plans.

VI. System considerations & Future Work

The architecture of the proposed WSN could include many low-cost emitters/readers, installed in a field and around them, multiple, backscatter sensors can be spread. Working in cells that contain groups of tags, each tag can backscatter information to the receiver at a specific subcarrier frequency. The tags inside each cell will employ frequency-division-multiple-access (FDMA) scheme, whereas the emitters/readers could operate in a time-division-multiple-access (TDMA) scheme. Using the above concept the development of a backscatter sensor network, could include hundreds of low-cost tags.

The classic WSN nodes utilize duty cycling operation in order to decrease the power consumption thus extending WSN lifetime. In this work, the tag was designed such that as low as possible power and the utilization of duty cycling could further decrease the required energy requirements. In [16] was demonstrated that the power consumption of a similar proposed backscatter WSN is lower than a ZigBee-type WSN. ZigBee sensors are based on IEEE 802.15.4 communication

protocol and are widespread for wireless area networks with small digital radios [33].

Future work will focus on sensing and communication measurements and on further deceasing the overall cost of the sensor node. A future challenge is also to design an RF electromagnetic energy harvester to combine all the different forms of ambient energy availability. The communication range of the above deployment can be extended by the following modifications. First, it is possible to use circular polarized and directive antennas instead on the monopoles at the receiver and the reader. The antennas would be designed and fabricated on the same substrate with a proper distance between them in order to maximize gain and keep mutual coupling between them at low level. With circular polarization the alignment between the reader/emitter antenna and the tag will have less effect. Secondly, the RF front-end dipole antenna could be replaced with a better gain antenna. This work is a first attempt to design a low-cost and low-power leaf sensor for agriculture and specific sensing plant measurements will be prepared in the future. The proposed sensor must be calibrated for different values on relative humidity and soil moisture for a specific type of plant. Finally, the cost of the tag can be reduced by replacement of the super capacitor and the solar panel with a cheaper option.

VII. Conclusion

In this paper a novel backscatter leaf sensing system for agricultural purposes was presented. Specifically, it includes a sensor for leaf canopy temperature measurements and it can be used for water stress measurements on plants. The sensor node has low-power consumption of only 20 μW and is supplied by a solar panel without need of battery. Morse code modulation was used for the wireless communication with a low-cost SDR receiver by backscattering RF signals from a carrier emitter. The proposed system is part of the backscatter WSN for agriculture with a small cost per sensor node. It is suitable for distributed monitoring of environmental parameters in largescale, precision agriculture applications.

Acknowledgment

The authors would like to thank Alexios Costouri and all members of Microwave Lab, Heriot-Watt University, Edinburgh, UK for their help in various steps throughout this work.

References

[1] S. Ivanov, K. Bhargava, and W. Donnelly, "Precision farming: Sensor analytics," *IEEE Intelligent Systems J.*, vol. 30, no. 4, pp. 76–80, Jul. 2015.

[2] L. Ruiz-Garcia, L. Lunadei, P. Barreiro, and I. Robla, "A review of wireless sensor technologies and applications in agriculture and food industry: state of the art and current trends," *Molecular Diversity Preservation International Open Access Sensors J.*, vol. 9, no. 6, pp. 4728–4750, Jun. 2009.

[3] C. Yu, Y. Cui, L. Zhang, and S. Yang, "Zigbee wireless sensor network in environmental monitoring applications," in *Proc. IEEE Conf. on Wireless Commun. Networking and Mob. Comput. (WiCOM)*, Binjiang, China, Sept. 2009, pp. 1–5.

[4] N. Fahmi, S. Huda, E. Prayitno, M. U. H. Al Rasyid, M. C. Roziqin, and M. U. Pamenang, "A prototype of monitoring precision agriculture system based on WSN," in *Proc. IEEE Int. Sem. on Intelligent Technology and Its Applications (ISITIA)*, Surabaya, Indonesia, Aug. 2017, pp. 323–328.

[5] V. Palazzari, P. Mezzanotte, F. Alimenti, F. Fratini, G. Orecchini, and L. Roselli, "Leaf compatible eco-friendly temperature sensor clip for high density monitoring wireless networks," *Cambridge Univ. Press Wireless Power Transfer*, vol. 4, no. 1, pp. 55–60, Feb. 2017.

[6] H.-D. Seelig, R. J. Stoner, and J. C. Linden, "Irrigation control of cowpea plants using the measurement of leaf thickness under greenhouse conditions," *Springer J. Irrigation Science*, vol. 30, no. 4, pp. 247–257, Jul. 2012.

[7] *SG-1000 Leaf Sensor*, AgriHouse Inc., 2017. [Online]. Available: https://www.biocontrols.com/Leaf%20Sensor/SG-1000softwareV1.pdf

[8] N. Abraham, P. Hema, E. Saritha, and S. Subramannian, "Irrigation automation based on soil electrical conductivity and leaf temperature," *Elsevier Agricultural Water Management J.*, vol. 45, no. 2, pp. 145–157, Jul. 2000.

[9] N. Patel, A. Mehta, and A. Shekh, "Canopy temperature and water stress quantificaiton in rainfed pigeonpea (Cajanus cajan (L.) Millsp.)," *Elsevier, Agricultural and Forest Meteorology*, vol. 109, no. 3, pp. 223–232, Sep. 2001.

[10] R. Pearcy, O. Bjorkman, A. Harrison, and H. Mooney, "Photosynthetic performance of two desert species with C4 photosynthesis in Death Valley, California," *Carnegie Institute Year Book*, vol. 70, pp. 540–550, 1971.

[11] G. Hornero, J. E. Gaitán-Pitre, E. Serrano-Finetti, O. Casas, and R. Pallas-Areny, "A novel low-cost smart leaf wetness sensor," *Elsevier, Computers and Electronics in Agriculture*, vol. 143, pp. 286–292, Dec. 2017.

[12] *PHYTOS 31, Dielectric Leaf Wetness Sensor, product manual*, Decagon Devices, Inc., 2016. [Online]. Available: http://library.metergroup.com/Manuals/10386_Leaf%20Wetness%20Sensor_Web.pdf

[13] A. P. Sample, D. J. Yeager, P. S. Powledge, A. V. Mamishev, and J. R. Smith, "Design of an RFID-based battery-free programmable sensing platform," *IEEE Trans. Instrum. Meas.*, vol. 57, no. 11, pp. 2608–2615, Jun. 2008.

[14] S. D. Assimonis, S. N. Daskalakis, and A. Bletsas, "Sensitive and efficient RF harvesting supply for batteryless backscatter sensor networks," *IEEE Trans. Microw. Theory Techn.*, vol. 64, no. 4, pp. 1327–1338, Apr. 2016.

[15] S. N. Daskalakis, S. D. Assimonis, E. Kampianakis, and A. Bletsas, "Soil moisture scatter radio networking with low power," *IEEE Trans. Microw. Theory Techn.*, vol. 64, no. 7, pp. 2338–2346, Jun. 2016.

[16] E. Kampianakis, J. Kimionis, K. Tountas, C. Konstantopoulos, E. Koutroulis, and A. Bletsas, "Wireless environmental sensor networking with analog scatter radio and timer principles," *IEEE Sensors J.*, vol. 14, no. 10, pp. 3365–3376, Oct. 2014.

[17] C. Konstantopoulos, E. Koutroulis, N. Mitianoudis, and A. Bletsas, "Converting a plant to a battery and wireless sensor with scatter radio and ultra-low cost," *IEEE Trans. Instrum. Meas.*, vol. 65, no. 2, pp. 388–398, Feb. 2016.

[18] S. F. Pichorim, N. J. Gomes, and J. C. Batchelor, "Two solutions of soil moisture sensing with RFID for landslide monitoring," *Multidisciplinary Digital Publishing Institute Sensors J.*, vol. 18, no. 2, p. 452, 2018.

[19] S. N. Daskalakis, A. Collado, A. Georgiadis, and M. M. Tentzeris, "Backscatter morse leaf sensor for agricultural wireless sensor networks," in *Proc. IEEE Sensors Conf.*, Glasgow, UK, Oct. 2017, pp. 1–3.

[20] J. J. Fahie, *A History of Electric Telegraphy, to the year 1837*. London: E. & FN Spon, 1884.

[21] J. G. Proakis and M. Salehi, *Digital Communications fifth edition, 2007*. McGraw-Hill Companies, Inc., New York, NY, 2008.

[22] *PIC16LF1459, USB Microcontroller with Extreme Low-Power Technology, product manual*, Microchip Technology Inc., 2014. [Online]. Available: http://www.microchip.com/downloads/en/DeviceDoc/40001639B.pdf

[23] *TS3002 1V/1uA Easy-to-Use Silicon Oscillator/Timer, product manual*, Silicon Laboratories, Inc., 2014. [Online]. Available: https://docs-apac.rs-online.com/webdocs/1257/0900766b812571eb.pdf

[24] *XC6504 Ultra Low Power Consumption Voltage Regulator, product manual*, Uorex Semiconductor, 2012. [Online]. Available: https://www.torexsemi.com/file/xc6504/XC6504.pdf

[25] C. Konstantopoulos, "Self-Powered Plant Sensor for Scatter Radio," Master's thesis, School of Electrical and Computer Engineering, Technical University of Crete, Greece, 2015.

[26] *TPL5010 Nano-power System Timer with Watchdog Function, product manual*, Instruments, Texas, 2015. [Online]. Available: http://www.ti.com/lit/ds/symlink/tpl5010.pdf

[27] *LMT84 Analog Temperature Sensor, product manual*, Instruments, Texas, 2017. [Online]. Available: http://www.ti.com/lit/ds/symlink/lmt84.pdf
[28] *ADG919 RF switch, product manual, product manual*, Analog Devices, 2016. [Online]. Available: http://www.analog.com/media/en/technical-documentation/data-sheets/ADG918_919.pdf
[29] K. Niotaki, A. Collado, A. Georgiadis, S. Kim, and M. M. Tentzeris, "Solar/Electromagnetic energy harvesting and wireless power transmission," *Proc. IEEE*, vol. 102, no. 11, pp. 1712–1722, Nov. 2014.
[30] *SP3-37 Flexible Solar Panel 3V @ 22mA, product manual*, PowerFilm, 2009. [Online]. Available: https://goo.gl/q5ECXh
[31] *NESDR SMArt Bundle-Premium RTL-SDR, product manual*, NooElec Inc., 2017. [Online]. Available: http://www.nooelec.com/store/nesdr-smart.html
[32] G. Radio, "The gnu software radio," *Available from World Wide Web: https://gnuradio. org*, 2007.
[33] P. Baronti, P. Pillai, V. W. Chook, S. Chessa, A. Gotta, and Y. F. Hu, "Wireless sensor networks: A survey on the state of the art and the 802.15.4 and Zigbee standards," *Elsevier, Computer Communications*, vol. 30, no. 7, pp. 1655–1695, May. 2007.